A Liquid Rocket Performance Model Based on Vaporization Interactions

D. L. KORS,* L. B. BASSHAM,† AND R. E. WALKER‡
Aerojet-General Corporation, Sacramento, Calif.

A performance model has been formulated that is similar to the Interagency Chemical Rocket Propulsion Group (ICRPG) Standard Performance Evaluation Procedure, but modified to include performance loss interactions based on liquid propellant vaporization theory. Vaporization limited combustion properties are used to evaluate rocket engine performance losses due to incomplete release of chemical energy, finite-rate limited gas expansion, and boundary-layer shear drag and heat transfer. A derivation of the performance loss methodology utilized is outlined. Performance test data are presented for liquid rocket engine systems utilizing both cryogenic LF_2/N_2H_4 blend propellants and earth-storable N_2O_4/A-50 propellants over a range of mixture ratios and nozzle exit area ratios. Application of the Vaporization Interaction Performance Model to the LF_2/N_2H_4 blend engine illustrates the improved definition of performance level and trends possible compared to the current ICRPG methods when engines that have unequal fuel and oxidizer vapor fractions are evaluated. Also, the capability of the Vaporization Interaction Performance Model to predict the observed performance of the N_2O_4/A-50 engine within the 3σ band of experimental measurements is apparent over the entire mixture ratio range tested for both sea level and altitude configurations.

Nomenclature

A-50	=	aerozine 50
BLL	=	boundary-layer loss, lbf sec/lbm
DL	=	divergence loss, lbf sec/lbm
ERL	=	energy release loss, lbf sec/lbm
KL	=	kinetic loss, lbf sec/lbm
I_{sp}	=	vacuum specific impulse, lbf sec/lbm
LF_2	=	liquid fluorine
MRDL	=	mixture ratio maldistribution loss, lbf sec/lbm
O/F	=	mixture ratio
P_c	=	chamber pressure, psia
T	=	temperature, °F
$\dot{w}$	=	mass flow rate, lbm/sec
X	=	fraction of mass flow rate vaporized, %
ΔF_{BLL}	=	boundary layer thrust decrement, lbf
$\lambda\epsilon$	=	area ratio
η_{DIV}	=	nozzle divergence efficiency

Subscripts

del	=	delivered value
e	=	over-all engine property
f	=	fuel or force
i	=	of ith stream tube
m	=	mass
n	=	number of stream tubes
o	=	oxidizer
ODE	=	one-dimensional equilibrium
ODK	=	one-dimensional kinetic
TDK	=	two-dimensional kinetic
theo	=	theoretical equilibrium performance
T	=	total engine property
v	=	vaporized property

Introduction

AN accurate analytical model for prediction, correlation, and extrapolation of liquid rocket performance has been an objective of the industry from its inception. A significant step toward achieving this goal was realized in 1968 when the ICRPG Performance Standardization Working Group (PSWG) published their Liquid Propellant Thrust Chamber Performance Evaluation Manual.[1] This document describes the significant sources of performance inefficiencies and their interaction and recommends two alternative performance evaluation procedures, with reference computer programs, to evaluate the various interrelated performance losses.

The PSWG limited the scope of its initial effort to assembling the best relevant techniques existing at that time throughout the industry. This resulted in the selection of five reference computer programs to evaluate performance of liquid propellant thrust chambers. These reference programs permit all the primary performance losses except the energy release loss (ERL) to be evaluated by inputting the appropriate design and operating variables. The ERL was considered to be of such a complex nature that it could not adequately be modeled by available analytical techniques. Therefore, an interim empirical procedure first postulated by Valentine and Pieper[2,3] was adopted. This procedure was a step beyond the classical $c^* - C_f$ performance model, and modeled the effect of incomplete energy release by reducing the input values for propellant heats of formation to the reference thermochemical computer programs.

This lack of a mechanistic characterization of the ERL was one of the more serious recognized limitations of the ICRPG Standard Performance Evaluation Procedure. Without this capability the model is somewhat limited in application as a prediction tool for new injector designs. The energy release potential of a new injector can only be assessed by estimating its similarity by inspection to another design that has been previously tested and an empirical reduced heat of formation value determined. However, the ability to estimate energy release differences by inspection does not result in comparable precision to that obtained from using the reference computer programs to evaluate the other component performance losses.

Also, the model may be limited in its ability to extrapolate from one nozzle area ratio to another for thrust chambers with incomplete propellant vaporization. This limitation results since the actual interaction between the ERL and the other component performance losses cannot properly be assessed without considering the effects of incomplete pro-

Presented as Paper 69-470 at the AIAA 5th Propulsion Joint Specialist Conference, U. S. Air Force Academy, Colo., June 9–13, 1969; submitted June 6, 1969; revision received July 31, 1969.

* Manager, Fluid Dynamics. Member AIAA.
† Senior Staff, Fluid Dynamics.
‡ Engineer, Fluid Dynamics.

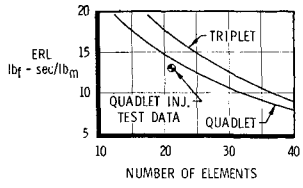

Fig. 1 Effect of number of elements on energy release loss.

pellant vaporization, which may lead to a different mixture ratio in the vapor. Incomplete energy release has a significant influence on kinetic loss calculations, and a slight influence on boundary-layer and two phase flow loss calculations.[1] However, to evaluate the significant effect that energy release has on kinetic loss calculations, the present ICRPG model assumes that the energy release defect can be characterized by an enthalpy reduction in the combustion gases. If in actuality the energy release deficiency is largely due to vaporization-limited combustion, the kinetic loss would be quite different from the value calculated with the assumption that the combustion products are completely vaporized but at a reduced enthalpy.

Extensive correlation of test data with a semiempirical vaporization model at Aerojet-General has indicated that most conventional liquid rocket combustion processes are indeed vaporization-limited. Therefore a revision of the present ICRPG performance model has been developed to incorporate vaporization-limited energy release performance interactions.

Vaporization Energy Release Model

The processes occurring in a liquid propellant thrust chamber can be classified into three general categories: atomization/vaporization, propellant mixing, and chemical reaction. Typical ranges of ERL, attributable to each of these processes are shown in Table 1. The propellant mixing process loss is usually in the 0 to 2% ERL range, since most state-of-the-art thrust chambers either have unlike impinging streams designed for effective intraelement mixing using criteria similar to the JPL mixing formula[4] or mixing is achieved by selective interelement mixing. Interelement mixing, which is enhanced by proper spatial orientation, is sometimes important for unlike impinging streams when stream separation occurs[5,6] and is always necessary for like impinging elements. Chemical reaction rates are usually not rate-limiting in normal thrust chamber combustion processes[7] but may be quite significant if combustion takes place at extreme variations from the stoichiometric condition.[8] Therefore, it is postulated that the atomization/vaporization process is usually the rate-limiting combustion process for most liquid propellant thrust chambers. In fact, the 0–8% ERL range is not wide enough to include the vaporization ERL for coarsely atomized streams in conjunction with short combustion chamber lengths.

A vaporization model originally developed by Priem and Heidmann[7] was selected as the basic formulation. The Beltran modification,[9] which accounts for the decomposition reaction of hydrazine base fuels, was included into the model. Unpublished empirical data from both cold and hot firing tests have been developed into semiempirical atomization formulations at Aerojet-General to account for injection design parameters such as impingement angle, momentum ratio, stream area ratio, and element type.

The model, as developed by Priem,[7] solves the combined energy, momentum, and mass transfer processes acting on a statistically defined droplet distribution. Functional relationships between the combustion related variables and vaporized propellants were generated using an interative computer solution of the various transfer processes. These solutions resulted in simplified equations relating chamber pressure, injection velocity, chamber geometry, orifice diameter, propellant combination, and injection temperature to thrust chamber performance.

The basic computer model solves simultaneously the heat transfer, mass transfer, and aerodynamic momentum transfer (drag) between the combustion gas and the liquid droplet. Heat input to the droplet raises the liquid droplet temperature and superheats the vapor droplet mantle. The heat flux is influenced by differential velocity between the droplet and the surrounding gas, chamber pressure, thermal transport properties of the propellant, and vapor mantle thickness surrounding the droplet. With hydrazine base fuels, in the region where droplet relative velocities are low, the two flame decomposition reaction is the heat source of the vaporization process.[9] Residence time of the droplet is determined by solving simultaneously the mass transfer, the heat-transfer, and the ballistic equations using empirical drag coefficients. Those droplets that are vaporized prior to the nozzle throat station are assumed to release their chemical energy by gas phase reactions with the other vaporized propellant; a total summation on a mass basis is then a measure of the thrust chamber energy release efficiency. The formulation of the ERL from the vaporization relationships is summarized in the following. X_o and X_f are determined from vaporization analysis;

$$(O/F)_v = (O/F)_e \cdot X_o/X_f \tag{1}$$

$$X_T = (X_o \dot{w}_{oe} + X_f \dot{w}_{fe})/\dot{w}_T \tag{2}$$

$$\text{ERL} = I_{\text{sp theo}_{(O/F)_e}} - I_{\text{sp theo}_{(O/F)_v}} \cdot X_T \tag{3}$$

To date inadequate treatment of droplet size distributions in a hot firing environment has compromised the utility of vaporization models. Work is progressing in this area[10,11] but solutions which supply completely accurate analytical predictions are not yet available. This problem has been circumvented at Aerojet-General by empirically determining effective droplet sizes. Using the functional relationships developed by Priem, effective droplet sizes and distributions have been backed out of experimental engine data covering a wide variety of operating conditions. Droplet sizes of this sort do not represent actual sizes or distributions, and contain whatever deficiencies are implicit in the original model. However, experience indicates that the model has remained valid over a wide range of design and operating points. The design conditions correlated with the model are 1) propellant combinations: cryogenic, earth storable, space storable; 2) propellant state: liquid/liquid, liquid/gas; 3) injector element types: doublets, triplets, quadlets, pentads, micro-orifice (HIPERTHIN§), co-axial, vortex, showerhead; and 4) thrust/element: 0.1 to 40,000 lbf.

The obvious output for such a model is predicted ERL as a function of design parameters, propellant combination, and operating conditions. Figures 1 and 2 illustrate the applications of the vaporization ERL model for determining the effect of number of elements and chamber length on the ERL value. In addition to these obvious direct applications of the vaporization model, there are significant performance interactions that result from consideration of vaporization-limited combustion. The vaporization model

Table 1 Energy release loss (ERL) contributions

Process	ERL, %
Propellant mixing	0–2%
Chemical reaction	<1%
Atomization/vaporization	0–8%

§ Acronym (High Performance Throttlable Injector) for an advanced injector protected under Patent 3,413,704 and others by Aerojet-General Corp., Sacramento, Calif.

output parameters, vaporized mixture ratio $(O/F)_v$ and vaporized mass fraction X_T are the basic inputs that affect the performance loss interactions, as discussed in the next section.

Vaporization Interaction Performance Model

Using the vaporization model output parameters of mixture ratio $(O/F)_v$ and mass fraction (X_T), the following formulation is defined to account for the effects of vaporization interaction on delivered performance:

$$I_{sp_{del}} = \sum_{i}^{n} \left[I_{sp\ TDK(O/F)_{vi}} \frac{\dot{w}_{vi}}{\dot{w}_T} \right] - \frac{\Delta F_{BLL}}{\dot{w}_T} \qquad (4)$$

Equation (4) has not only the vaporization effects included, similar to the ERL formulation of (3), but in addition makes allowance for the effects of the other performance losses on delivered specific impulse. In fact, Eq. (4) is in a form that lends itself directly to evaluation by the ICRPG recommended two-dimensional kinetic (TDK) computer program,[12] which can be used to evaluate the first term on the right-hand side of Eq. (4). This TDK program concomitantly calculates the effect of kinetic-rate-limited gas expansion, nozzle divergence loss due to nonaxially directed exit momentum, and mixture ratio maldistribution loss caused by a two stream tube expansion at different mixture ratios. The last term on the right-hand side of Eq. (4) accounts for the viscous, nonadiabatic boundary-layer flow which can be evaluated by the ICRPG recommended turbulent boundary layer computer program.[13] Utilization of these two computer programs will permit a predicted delivered specific impulse to be calculated with a methodology identical to the ICRPG Standard Performance Evaluation Procedure[1] except for the above defined additional influence of vaporization interaction criteria.

A formulation similar to Eq. (4) can be defined in a form that will lend itself to evaluation by a methodology similar to the ICRPG Simplified Performance Evaluation Procedure.[1]

$$I_{sp_{del}} = \sum_{i}^{n} \left[I_{sp\ ODK(O/F)_{vi}} \frac{\dot{w}_{vi}}{\dot{w}_T} \right] \eta_{DIV} - \frac{\Delta F_{BLL}}{\dot{w}_T} \qquad (5)$$

Equation (5) is in a form that will permit use of 1) the ODK computer program[14] to determine $I_{sp_{ODK\ (O/F)_{vi}}}$; 2) the turbulent boundary layer computer program[13] to determine $\Delta F_{BLL}/\dot{w}_T$; and 3) the divergence loss charts in the ICRPG Performance Manual[1] to determine the η_{DIV} multiplier. These are the procedures recommended by the ICRPG[1] for the Simplified Performance Evaluation Procedure. In the following discussion, each loss is defined independently in order to show how the vaporized propellant parameters influence the loss analysis.

The energy release loss (*ERL*) accounts for the performance reduction as a result of incomplete vaporization, mixing, and chemical reaction. As described in the previous section this loss is evaluated by determining the mass defect caused by unvaporized propellant and the effect of the vaporized mixture ratio on the thermochemical performance output. Using one-dimensional equilibrium (ODE) conditions as the baseline or maximum achievable performance, the energy release loss at any nozzle expansion ratio can be found by subtracting the product of the total percent mass of propellant vaporized and the ODE specific impulse at the vaporized mixture ratio from the ODE specific impulse at the liquid propellant mixture ratio. Using the ODE notation, Eq. (3) becomes

$$\text{ERL} = I_{sp\ ODE(O/F)} - I_{sp\ ODE(O/F)_V} \cdot (\dot{w}_v/\dot{w}_T) \qquad (6)$$

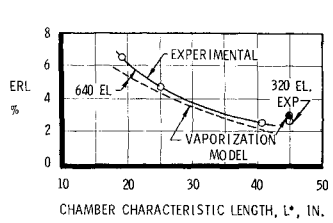

Fig. 2 Effect of L^* on energy release loss.

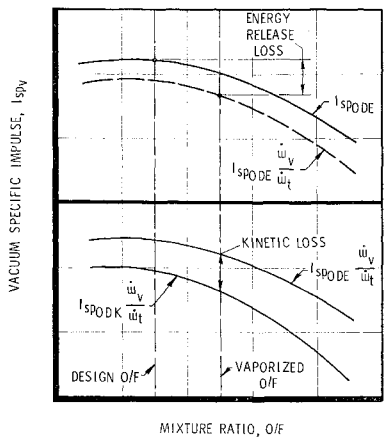

Fig. 3 Effect of vaporization on ERL and kinetic loss.

The upper part of Fig. 3 illustrates the ERL for a thrust chamber with a higher fraction of oxidizer vaporized than fuel. Consequently, its vaporized mixture ratio is shifted to a higher value and the total performance loss includes both the effect of the unvaporized propellant mass defect and the performance shift due to a change in mixture ratio.

For an engine with several stream tubes of different mixture ratios or atomization/vaporization characteristics, this process is used for each stream tube and the results are flow rate weight summed to give the total loss. Therefore Eq. (6) can be generalized to the following notation:

$$\text{ERL} = \sum_{i}^{n} \frac{[I_{sp\ ODE(O/F)_i}\, \dot{w}_i - I_{sp\ ODE(O/F)_{VI}}\, \dot{w}_{vi}]}{\dot{w}_T} \qquad (7)$$

The mixture ratio maldistribution loss (*MRDL*) accounts for the performance degradations due to nonhomogeneous combustion products on a macroscopic scale. The loss may be induced intentionally, as with barrier or fuel film cooling or may be unintentional as a result of nonuniform injector hydraulics. The mixture ratio maldistribution loss is calculated using a stream tube technique. The ODE specific impulse for the individual stream tubes at the stream tube mixture ratios are summed on a fractional mass flow rate and then subtracted from the ODE specific impulse at the over-all mixture ratio to define this loss. This performance loss definition is similar to the notation used in the present ICRPG Standard Performance Evaluation Procedure[1] for MRDL calculations that are beyond the two stream tube capability of the reference computer program. Again, using ODE as the reference condition, the MRDL is defined by the following relationship:

$$\text{MRDL} = I_{sp\ ODE(O/F)_e} - \sum_{i}^{n} I_{sp\ ODE(O/F)_i} \cdot \frac{\dot{w}_i}{\dot{w}_T} \qquad (8)$$

where the ith stream tube refers to discrete zones of flow whose mixture ratio is calculable by known injector hydraulic parameters.

The kinetic losses (*KL*) account for performance reduction from the equilibrium condition due to finite chemical reaction and relaxation rates of the species present in the exhaust gas during the nozzle expansion process. The kinetic loss is defined by considering the mass flow rate summed ODE performance at the stream tube vaporized mixture ratios as the reference point. The ODK performance is evaluated at the vaporized mixture ratio for each of the individual stream tubes and summed over the n stream tubes; this value is then subtracted from the ODE performance to obtain the kinetic

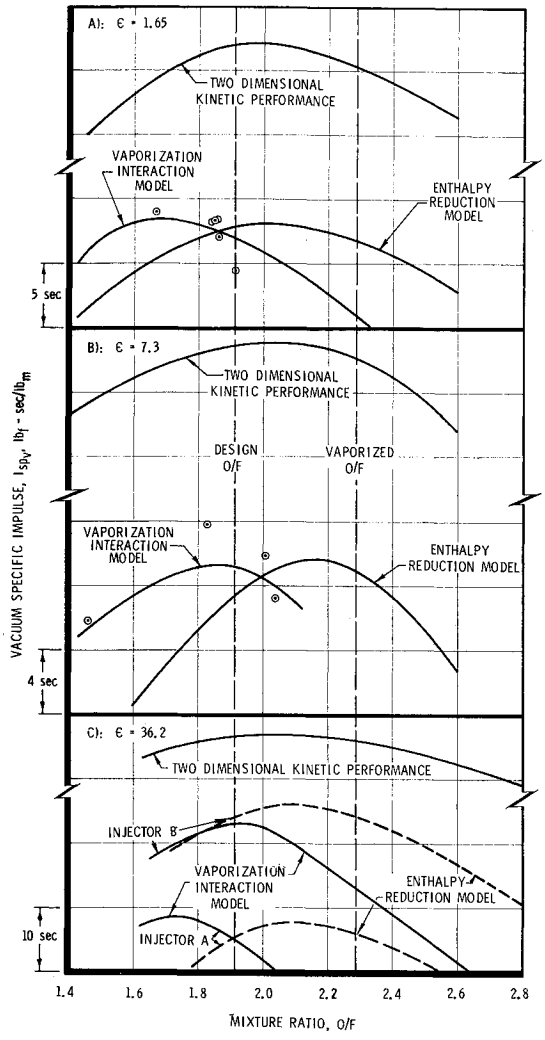

Fig. 4 LF_2/N_2H_4 blend performance, P_c = 100 psia.

loss. Again it is emphasized that both the kinetic and ODE performance must be evaluated at the vaporized mixture ratio and mass flow rate rather than at the liquid propellant mixture ratio, since the vaporized parameters represent the actual composition of the exhaust gases. The unvaporized portion of the propellants is actually in a nongaseous state and cannot be considered in the exhaust gas expansion process, other than the two phase flow velocity and thermal lag effects which are beyond the scope of this paper. The mathematical representation of this definition is

$$\mathrm{KL} = \sum_{i}^{n} [I_{\mathrm{sp\ ODE}(O/F)_{\mathrm{VI}}} - I_{\mathrm{sp\ ODK}(O/F)_{\mathrm{VI}}}] \frac{\dot{w}_{vi}}{\dot{w}_T} \qquad (9)$$

This loss is depicted in the lower part of Fig. 3 for a unit that is fuel vaporization limited. The I_{sp} curves have been adjusted for the mass fraction of propellant vaporized, since the loss is a result of only the processes related to the vaporized propellants. Definition of the KL does not include the effect of shifts from design point O/F to vaporized O/F, since this effect is evaluated with the energy release loss.

The boundary layer loss (BLL) accounts for the degradation of performance due to shear drag and heat loss at the boundary of the thrust chamber. The boundary-layer loss is evaluated using the vaporized performance combustion properties in the outer stream tubes. Again, the vaporized composition is considered rather than the composition based on over-all propellant flow rates. Using a suitable evaluation procedure a ΔF_{BLL} is calculated and divided by the total propellant flow rate to determine the BLL;

$$\mathrm{BLL} = (\Delta F_{\mathrm{BLL}})_{(O/F)}/\dot{w}_T \qquad (10)$$

The nozzle divergence loss (DL) accounts for the decrease in thrust due to nonaxially directed momentum at the nozzle exit and the nonplanar sonic surface. In most cases this loss is affected insignificantly by the variance of the vaporized mixture ratio from the over-all liquid flow mixture ratio. Therefore, no vaporized mixture ratio notation is included in the definition of the divergence loss. This performance loss when evaluated by itself can usually be expressed in terms of a divergence efficiency, η_{DIV}, which modifies the delivered or actual thrust,

$$\mathrm{DL} = I_{\mathrm{sp_{del}}}[(1 - \eta_{\mathrm{DIV}})/\eta_{\mathrm{DIV}}] \qquad (11)$$

The analytically predicted specific impulse of a vaporization-limited rocket engine can now be evaluated by subtracting the above defined performance losses from the ODE theoretical condition

$$I_{\mathrm{sp_{del}}} = I_{\mathrm{sp_{del}}} - \mathrm{ERL} - \mathrm{MRDL} - \mathrm{KL} - \mathrm{BLL} - \mathrm{DL} \qquad (12)$$

Substituting Eqs. (7–11) for the five performance loss terms of Eq. (12) and cancelling like terms, the final formulation already defined by Eq. (5) is obtained.

Application of Model

The model is applied to two similar sized thrust chambers using propellant combinations having significantly different vaporization relationships, and the results are compared to performance predictions using the standard ICRPG performance model which bases energy release loss on propellant enthalpy reduction. First, an engine system that uses the space-storable LF_2/N_2H_4 blend propellant combination was selected in order to illustrate the effect of a large mixture ratio shift when vaporized propellant properties are assessed. This system would be expected to show a significant vaporization interaction effect. The other engine system selected for evaluation used the earth storable N_2O_4/A-50 propellant combination which characteristically has more nearly equal oxidizer and fuel vaporization rates. This system was calculated to have only a minor vaporized mixture ratio shift, and would not be expected to show a significant vaporization interaction effect. The systems selected for this paper are Aerojet-General Transtage size configurations with design and calculated vaporized characteristics tabulated in Table 2.

An examination of the LF_2/N_2H_4 blend data will show the relative ability of the two models to predict performance over a range of mixture ratio for a fuel vaporization limited engine. Low-area-ratio, ϵ = 1.65, test data are presented in Fig. 4a, along with the predicted performance based on the ICRPG enthalpy reduction model and the vaporization interaction model. Energy release losses calculated by the enthalpy reduction model and the vaporization interaction model were correlated with test data about the design point mixture ratio of 1.91. However, when this design-point

Table 2 Engine design characteristics

Propellant combination	LF_2/N_2H_4 blend	N_2O_4/A-50
F, lbf	7000	8000
P_c, psia	100	105
X_o	99.5	98.4
X_f	83.6	98.5
$(O/F)_e$	1.91	2.00
$(O/F)_v$	2.27	2.00

correlation for both models was extended over a range of mixture ratios, a divergence in the predicted specific impulse-mixture ratio relationship resulted. Two-dimensional kinetic performance is given since it is the reference that was used by both models. The ability of the vaporization interaction model to represent the data more closely over the mixture ratio range is a result of the vaporized O/F being higher than the design mixture ratio (see Table 2), which has the effect of shifting the peak delivered performance to a lower O/F.

Altitude predictions based on ERL values verified by the $\epsilon = 1.65$ test data were made for a nozzle configuration with an intermediate area ratio of 7.3. This configuration was test-fired and the results together with altitude predictions using the two models are given in Fig. 4b over a range of mixture ratios. Again, the vaporization interaction model more closely correlates the test data and defines the higher performance potential at the lower mixture ratio. At the 1.46 mixture ratio test condition the predicted I_{sp} using the enthalpy reduction model was 9.0 sec lower than the measured I_{sp}, whereas the prediction using the vaporization interaction model was within 0.5 sec of the test data.

The importance of accurate performance prediction over a wide range of mixture ratio is illustrated by extrapolation of the low-area-ratio performance data to a high-area-ratio configuration. For the LF_2/N_2H_4 blend program this nozzle area ratio was 36.2. Two injectors, denoted here as A and B have extrapolated altitude performance as shown in Fig. 4c, using both the enthalpy reduction model and the vaporization interaction model. Kinetic performance is given for comparison. The lower performing unit, injector A, develops peak performance at an O/F of 1.75 using vaporization interaction model scaling, and at 2.1 using enthalpy reduction model scaling. This characteristic shift in optimum mixture ratio is similar to the altitude performance shift noted for the 7.3 area ratio test data shown in Fig. 4b. It is apparent that the selection of an optimum design point mixture ratio based on the vaporization interaction model would be considerably different from the value selected based on the enthalpy reduction model.

The higher performing unit, injector B, also was tested with a $\epsilon = 1.65$ nozzle. Extrapolating its data to the $\epsilon = 36.2$ condition over a range of mixture ratios results in the curves shown in Fig. 4c. The figure shows that the disparity in the optimum O/F is reduced since the vaporized mixture ratio of the higher performing injector is closer to the design value. As injector performance is increased through greater fuel vaporization efficiency and interelement mixing, the two-dimensional kinetic performance will more nearly define the optimum O/F.

The other propellant combination considered was N_2O_4/A-50, with an injector design that resulted in nearly equal vaporized propellant percentages for both the fuel and oxidizer (see Table 2). For these conditions the vaporization interaction model and enthalpy reduction model should predict approximately the same performance characteristics. Test data from the N_2O_4/A-50 engine at an area ratio of 1.0:1 is shown in Fig. 5a for seven injectors. Also shown in Fig. 5a is the predicted performance using the two models. For the enthalpy reduction model the energy release efficiency at the average mixture ratio was used to extrapolate performance over the mixture ratio range. For the vaporization interaction model the ERL was directly calculated over the mixture ratio range and did not require test data input. Excellent agreement is shown with both analysis techniques. Both models predict within the 3σ experimental range over the entire mixture ratio band, with a maximum disparity of one second at mixture ratios outside the nominal operating range.

Extrapolating these low-area-ratio data to 40:1 area ratio vacuum conditions, results in the curves shown in Fig. 5b. Again, the two models predict almost identical trends with a

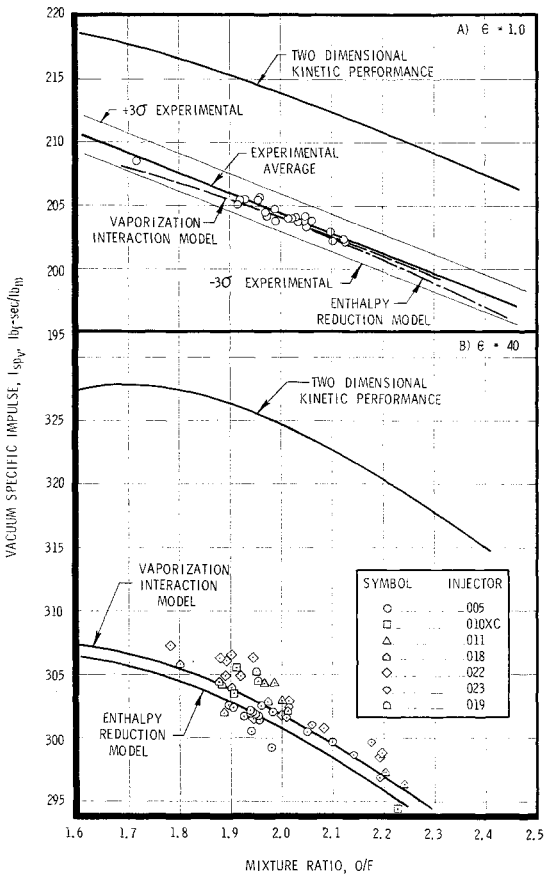

Fig. 5 N_2O_4/A-50 transtage performance, $P_c = 105$ psia.

maximum deviation of only 1.0 sec of I_{sp} from the empirical average. Similarity between the unvaporized mass defect and the kinetic performance curve is a result of the absence of any significant shift between the vaporized mixture ratio and the design mixture ratio (see Table 2).

Conclusions

The vaporization interaction model described here represents a significant improvement in modeling liquid rocket thrust chamber performance. Consideration of vaporized mass flow and mixture ratio parameters is particularly significant for thrust chambers having a disparity in the vaporized propellant fraction between the oxidizer and fuel components. For all conventional liquid rocket thrust chambers, the vaporization interaction performance model in conjunction with the ICRPG performance loss evaluation programs is capable of determining the engine O/F for near optimum performance and the expected delivered specific impulse during the initial design phase of the program.

References

[1] Pieper, J. L., "ICRPG Liquid Propellant Thrust Chamber Performance Evaluation Manual," Rept. 178, Sept. 1968, Chemical Propulsion Information Agency.

[2] Valentine, R. S., Dean, L. E., and Pieper, J. L., "An Improved Method of Rocket Engine Performance Prediction," *Journal of Spacecraft and Rockets*, Vol. 3, No. 9, Sept. 1966, pp. 1409–1414.

[3] Pieper, J. L., Dean, L. E., and Valentine, R. S., "Effects of Chamber Energy Release Efficiency Upon Nozzle Performance," *Journal of Spacecraft and Rockets*, Vol. 4, No. 5, May 1967, pp. 700–702.

[4] Riebling, R. W., "Criteria for Optimum Propellant Mixing in Impinging Elements," *Journal of Spacecraft and Rockets*, Vol. 4, No. 6, June 1967, pp. 817–819.

[5] Kushida, R. and Hauseman, J., "Criteria for Separation of

Impinging Streams of Hypergolic Propellants," TM 33-395, July 15, 1968, Jet Propulsion Lab., Pasadena, Calif.

[6] Lawver, B. R., "An Experimental Study of N_2O_4/N_2H_4 Jet Separation Phenomena," Paper presented at the Fifth ICRPG Combustion Conference, Baltimore, Md., Oct. 1968.

[7] Priem, R. J. and Heidmann, M. F., "Propellant Vaporization as a Design Criteria for Rocket Engine Combustion Chambers," TR R-67, 1960, NASA.

[8] Anderson, R. E., "A Model for N_2O_4 Rich Reactions," Technical Paper 3 LRO, Dec. 1964, Aerojet General Corp., Sacramento, Calif.

[9] Beltran, M. R. et. al., "Liquid Rocket Engine Combustion Instability Studies," AFRPG TR 66-125, July 1966, Dynamic Science Corp., Monrovia, Calif.

[10] Dickerson, R., Tate, K., and Parsec, N., "Correlation of Spray Injector Parameters with Rocket Engine Performance," AFRPL TR 68-147, June 1968, Edwards, Calif.

[11] Matthews, B. J., Wuerken, R. F., and Harje, D. T., "Small Droplet Measuring Technique," AFRPL TR-68-156, Edwards, Calif.

[12] Kliegel, J. R. et al., "Two Dimensional Kinetic Nozzle Analysis Computer Program," AD 841200, July 1968, ICRPG Performance Standardization Working Group.

[13] Weingold, H. D. and Zupnik, T. F., "Turbulent Boundary Layer Nozzle Analysis Computer Program-TBL," AD 841202, July 1968, ICRPG Performance Standardization Working Group.

[14] Frey, H. M. et al., "One Dimensional Kinetic Nozzle Analysis Computer Program," AD 841201, July 1968, ICRPG Performance Standardization Working Group.

OCTOBER 1969 J. SPACECRAFT VOL. 6, NO. 10

Saturn V/S-IC Stage Base Thermal Environment

C. R. MULLEN* AND R. L. BENDER†
The Boeing Company, Huntsville, Ala.

This paper contains an analysis of the measured thermal and pressure environments in the base of the S-IC stage during the AS-501 and AS-502 flight tests. Base gas temperatures, radiation levels, and total heating rates were measured during both flights and base-mounted TV cameras on the AS-502 flight provided a visual observation of the base gas flowfield. These data indicate that significant radiation is contributed by hot gases being recirculated into the base. Radiation was the main source of heating, although convective heating on the engine nozzle extension was significant. Base flow deflectors on the AS-501 flight were removed for the AS-502 flight and produced a significant increase in AS-502 base heating. Comparisons of flight data with model test data indicate that model data are useful in defining base pressure, gas temperature, and effects of changing configuration but cannot be used directly to indicate magnitudes of convective or radiation heating for the prototype.

Introduction

THE Saturn V booster is the largest of the Saturn class vehicles developed by NASA/MSFC to implement the Apollo moon landing program. One of the areas of concern during the design and development of the Saturn V was the base region of the S-IC stage where significant heating was expected to occur during boost. A part of the Saturn V/S-IC stage development program conducted by The Boeing Company and NASA/Marshall Space Flight Center consisted of extensive base heating model tests, application of Saturn I and IB flight test data[1] and instrumenting of the first Saturn V flight vehicles to define the S-IC base environment to assure adequate base thermal protection.

The AS-501 and AS-502 flights on November 9, 1967 and April 4, 1968, respectively, produced a significant amount of S-IC base heating data.[2,3] The Saturn V/S-IC stage base configuration consists of five F-1 engines mounted in a cross-engine arrangement of four maneuverable engines around a fixed center engine (Figs. 1). The engines use LOX/RP-1 at a mixture ratio of 2.26:1. A heat shield is located 19 ft forward of the engine exits and base flow deflectors were located on the AS-501 around the periphery of the base to remove combustible gas mixtures from the base area and to cool the base. The flow deflectors were removed on AS-502. Turbopump exhaust gases were eliminated by exhausting them inside the F-1 engine nozzle from the 10:1 to 16:1 area ratio. This created a fuel rich gas mixture surrounding each of the engine exhaust flows. This paper describes the measured S-IC base heating environments and compares them with Saturn I and IB flight data and 1/45th-scale model test data.

Presented as Paper 69-318 at the AIAA 3rd Flight Test, Simulation, and Support Conference, Houston, Texas, March 10–12, 1969; submitted February 28, 1969; revision received July 1, 1969.

* Senior Group Engineer, Aerophysics. Member AIAA.
† Member of Aerophysics Group. Member AIAA.

Flight Instrumentation and Data Reduction

The instrumentation consisted of 6 radiation calorimeters, 19 total calorimeters, 14 gas temperature probes, 18 static pressure taps, 4 total pressure probes, and 2 differential pressure gages at the locations shown in Fig. 1.

The sensing surfaces of the heat shield total and radiation calorimeters were 0.17 in. and 0.55 in. in diameter, respectively, and were mounted so that the sensing surfaces of the total calorimeters and the sapphire windows of the radiation calorimeters were flush with the heat shield surface. The sapphire window on the radiation gage was protected from sooting by a nitrogen purge. The radiation and total calorimeters are asymptotic instruments with a constantan sensor surface coated with a high-emissivity black coating.[4,5] The calorimeters maintained a low wall temperature throughout flight with an "effective"[6] sensing surface temperature of approximately 610°R.

The heat shield gas temperature probes consisted of a 0.25-in. diam molybdenum single shield with a platinum rhodium thermocouple junction for the sensing surface. Gases were admitted to the sensing surface through four equally spaced